EARTHQUAK OBSERVATION ON TWO SUBMERGED TUNNELS AND NUMERICAL ANALYSIS

M. HAMADA

SUMMARY

Earthquake observation and numerical analyses were carried out on two submerged tunnels in Tokyo Port in order to study the dynamic characteristics of the behavior of the tunnels and the surrounding ground. By qualitative and quantitative examination on the observed records during two typical earthquakes it was clarified that the axial and the bending strains depended on the velocity and the acceleration of the earthquake motion, respectively and the flexible joints between tunnel elements had great effectiveness on the reduction of the dynamic strains of the tunnels.

INTRODUCTION

Recently in Japan earthquake resistant design of submerged tunnels has been done by the response displacement method, namely by considering ground displacement as the main effect of earthquake motion on tunnel's dynamic deformation. In case of application of the response displacement method to the earthquake resistant design engineers often find a lot of difficulties to exactly estimate the coefficient of subgrade reaction and the stiffness of the joints between tunnel elements which have a great influence of the stress evaluation.

Dynamic strains of tunnels, relative displacements of joints and acceleration of the surrounding ground were observed on two adjacent submerged tunnels during earthquakes to study the characteristics of the dynamic behavior of the tunnels as well as to examine the applicability of the response displacement method. Furthermore, the stiffness of the joints and the coefficient of the subgrade reaction were estimated by the comparison of the observed strains and the relative displacement with the analyzed ones.

EARTHQUAKE OBSERVATION ON TWO SUBMERGED TUNNELS

Outline of Two tunnels and Geophysical Condition

Two submerged tunnels, where the earthquake observation was conducted, had been constructed within a close distance of about 3.0 km in Tokyo Port as shown in figure 1. The lengthes of two tunnels (hereafter call as A and B) are 1035 m add 744 m, respectively. The tunnels consists of 9 (A-tunnel) and 6 (B-tunnel) reinforced concrete elements with flat rectangular cross-sections shown in Fig. 2 and the length of about 110 m. Each element is connected by flexible joints shown in Fig. 3. B-tunnel had much more flexible joints which are fabricated by only steel cables than A-tunnel where the joints are by steel shear keys and mortar concrete.

Observed Dynamic Strains and Accelerations

Professor of Ocean Civil engineering, Tokai University, Shizuoka, JAPAN

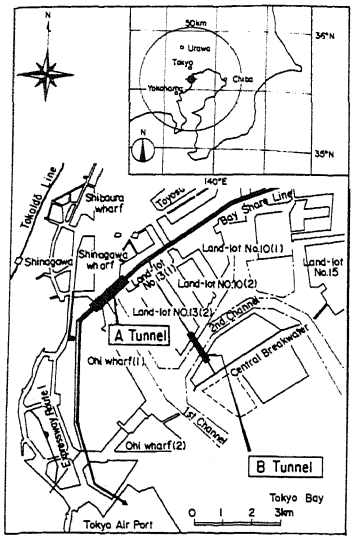

Fig. 1 Location of Two Submerged Tunnels

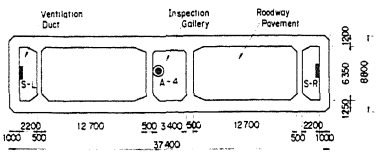

(a) A-Tunnel

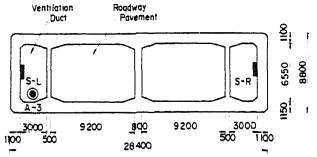

(b) B-Tunnel

Fig. 2 Cross-Section of Tunnels

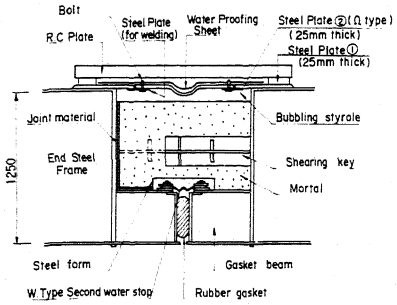

(a) A-Tunnel

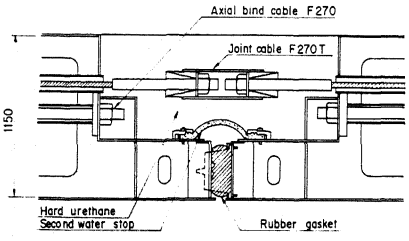

(b) B-Tunnel

Fig. 3 Flexible Joints

More than ten earthquakes with small ∿ medium intensity (the maximum accelerations of which were larger than 10 cm/sec^2) were observed. Fig. 5 shows an example of accelerations and dynamic strains recorded on B-tunnel during an earthquake which occured in the near sea of Izu-Penistsula (call as Izu-Earthquake). The magnitude, the epicentral distance and the depth of the focus were 6.7, 80 km and 10 km, respectively. the acceleration was observed on the Tertiary layer (A1) and on the ground surface (A2) in the axial direction (X) as well as in the lateral direction (Y). The strain due to the push-pull deformation of the tunnel (axial strin) and the strain due to the bending deformation around the vertical axis (bending strain) were calculated from strains in the axial direction observed on the inner surface of the both side walls as shown in Fig. 2. From the records shown in Fig. 2 the following results were obtained:

(a) Acceleration is large during 0 ∿ 40 sec of the records and high frequency vibration is dominant in this term. During the term after 40 sec long period components of 7.0 ∿ 8.0 sec are notable. The bending strains are

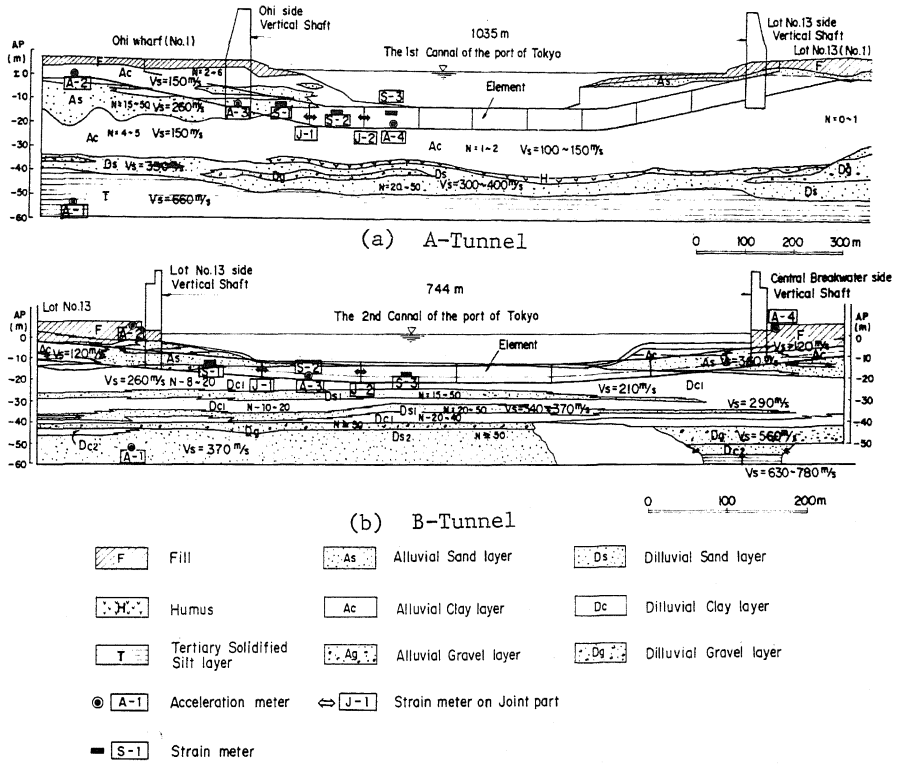

Fig. 4 Soil Profile and Location of Measuring Instruments

large during the former term of the record and short period components are dominant. On the contrary the axial strains are large during the later term and long period components are remarkable. The axial strains about 4 ∿ 5 times larger than the bending strains.

(b) From the similarity of the axial strains at three observation points (S1, S2 and S3) the push-pull deformation of the tunnel can be considered to be uniform along the tunnel axis. The bending strains at the three points have much differences to each other. It can be concluded that the local condition of the surrounding ground has much more influence on the bending deformation than on the push-pull deformation.

Correlation between Tunnel Strain and Ground Deformation

The ground displacements in the axial (u) and the lateral (v) directions, caused by the earthquake waves travelling apparently along the tunnel axis as shown in Fig. 6, can be written as;

$$u = f\left(t - \frac{x}{Vx}\right) \qquad v = g\left(t - \frac{x}{Vx}\right) \quad \cdots\cdots\cdots \quad (1)$$

where V_x and V_x' are the apparent phase velocities of each component which are assumed to be constant without respect to the frequency. The normal strain of the ground in the axial direction γ_{xx} is

$$\gamma_{xx} = \frac{\partial f}{\partial x} = -\frac{1}{Vx}\frac{\partial f}{\partial t} \quad \cdots\cdots\cdots (2)$$

and the curvature of the ground deformation $1/\rho = \frac{\partial^2 g}{x^2}$ is

$$\frac{1}{\rho} = \frac{\partial^2 g}{\partial x^2} = \frac{1}{V_x'}\frac{\partial^2 g}{\partial t^2} \quad \cdots\cdots\cdots (3)$$

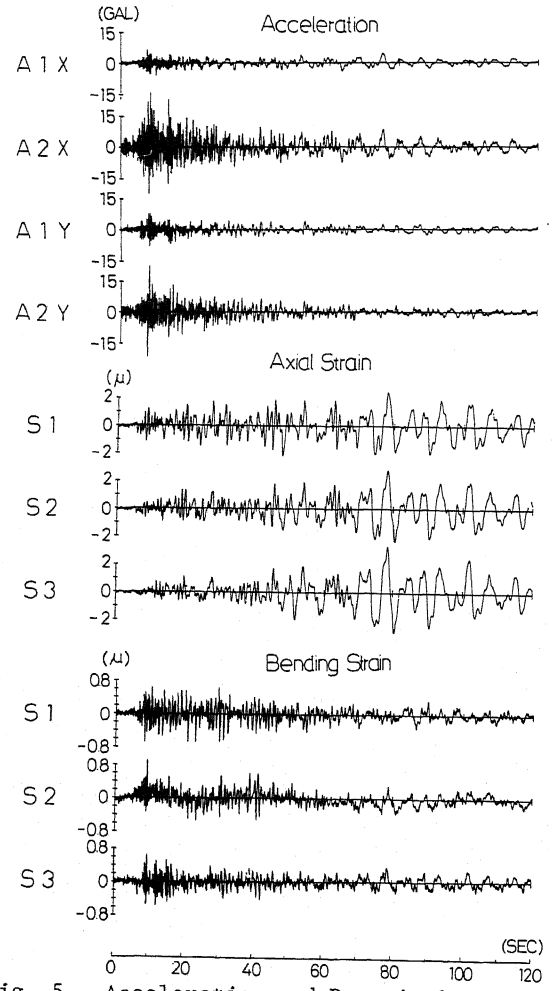

Fig. 5 Acceleration and Dynamic Strain of B-Tunnel during Izu-Earthquake

$\frac{\partial f}{\partial t}$ and $\frac{\partial^2 g}{\partial x^2}$ are the velocity and the acceleration of the particle motion.

Fig. 7 and 8 show the axial and the bending strains of two tunnels in a comparison with the velocity and the acceleration of the particle motion during two typical earthquakes. The first one, Izu-Earthquake mentioned previously, was caused by a shallow fault and has a distant epicenter. The second one, Ciba-Earthquake was caused by a deep fault in near field and the magnitude, the epicentral disdance and the depth of the fault were 6.1, 40 km and 80 km, respectively. The positive direction of accelerations, velocities and strains as well as the epicentral directions of two earthquakes are shown in Fig. 9. The following results can be obtained from Fig.7 and 8.

(a) The axial strains of the two tunnels have similar wave forms and spectra to the particle velocities of the earthquake motion. Furthermore, a close relationship can be found between the bending strains and the accelerations.

By considering the relation bewtween the curvature of ground deformation and the lateral acceleration in Eq.(3) and the direction of the lateral axes (Y) shown in Fig. 9, it can be understood that the bending strain should have same phase to the lateal acceration in A-tunnel and opposite phase in B-tunnel without respect to positive and negative of the

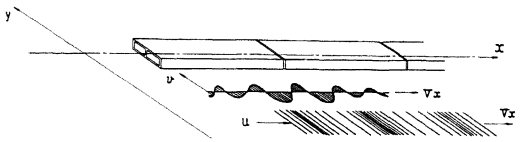

Fig. 6 Wave Travelling apparently along Tunnel Axis

apparent phase velocity. Furthermore, the axial strain should have same phase with the axial velocity in the both tunnels during Chiba-Earthquake, because the apparent phase velocities of the incident motion along the axes are negative, but opposite phase in A-tunnel during Izu-Earthquake because of the positive apparent phase velocity.

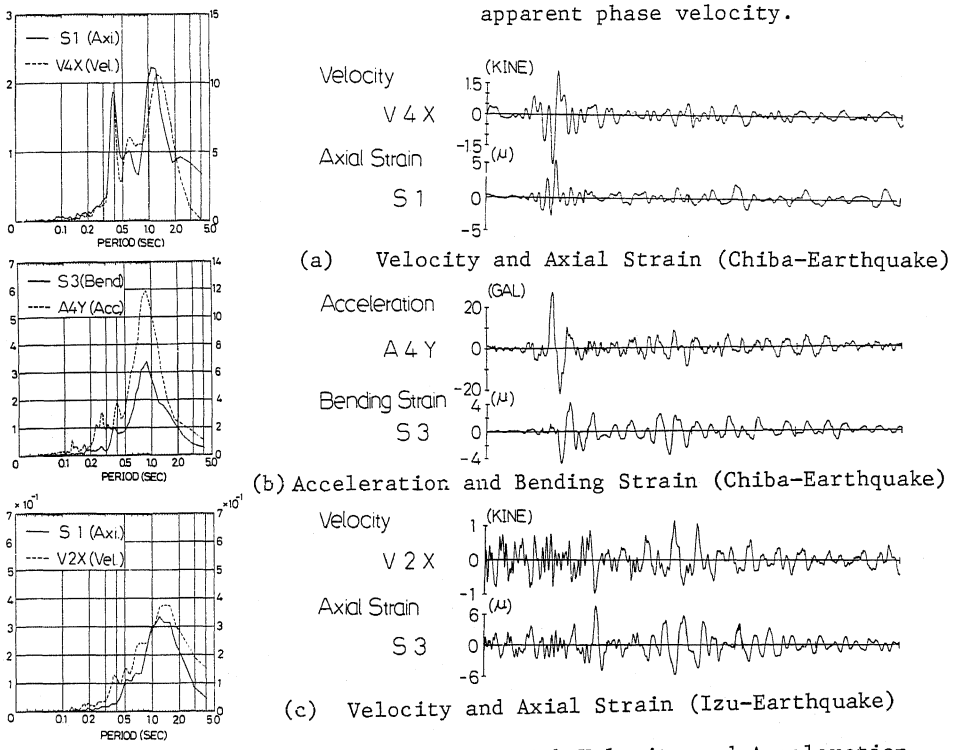

Fig. 7 Comparison of Dynamic Strains with Velocity and Acceleration (A-Tunnel)

(b) The relationship of the wave phases shown in Fig. 7 and 8 is well consistent with the above-mentioned consideration. For example, the axial strains of both tunnels have same phase with the axial particle velocities during Chiba-Earthquake shown in Fig. 7(a) and Fig. 8(a), while the bending strains have same phase in A-tunnel in Fig. 7(b) and opposite in B-tunnel in Fig. 8(b). Furthermore, the axial strain of A-tunnel has same phase with the velocity during Izu-Earthquke as shown in Fig. 7(c).

NUMERICAL ANALYSIS BY A SIMPLIFIED MODEL

Simple Numerical Model

Several numerical methods for the estimation of dynamic strains of submerged tunnels were already proposed on the basis of the concept of the response displacement method.(1) However in most of cases it is difficult

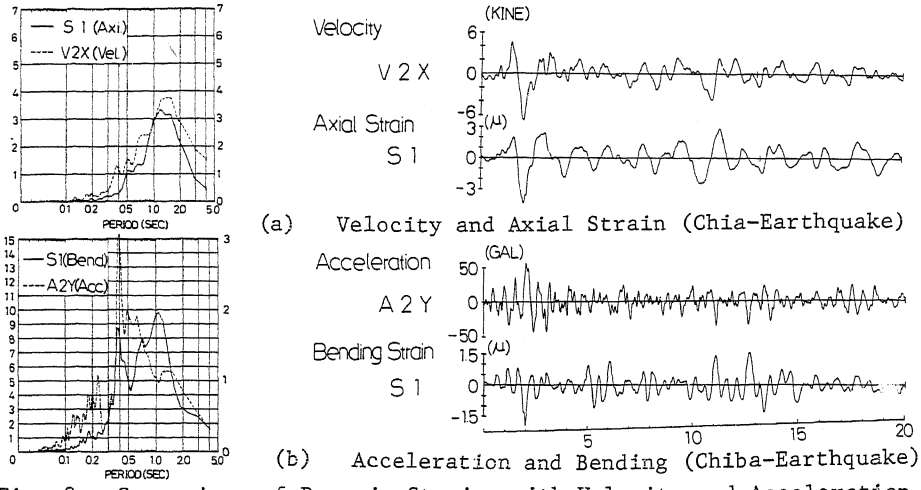

Fig. 8 Comparison of Dynamic Strains with Velocity and Acceleration (B-Tunnel)

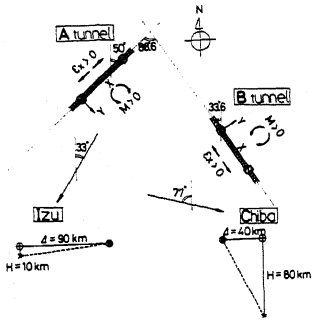

Fig. 9 Positive Directions of Tunnel Axies, Earthquake Motions, and Strains and Epicentral Directions

for the engineers to estimate exactly the ground deformation which is strongly influenced by the complicated geophysical condition in the large area along the tunnel axis as well as by the characteristics of the incident earthquake waves. And also there are some difficulties on the exact evaluation of the coefficient of the sub-grade reaction and the flexibility of joints between tunnel elements.

Therefore, in this paper a simple model was used to calculate approximate values of dynamic strains of tunnels and of relative displacement of joints. The assumptions are follows;

(a) The tunnel is consisted of a infinite chain of tunnel elements and joints as shown in Fig. 10.

(b) Only axial strain is calculated since it is generally much more dominant than the bending strain. The normal strain of the ground in the axial direction is uniform along the tunnel axis.

The dynamic strain of the tunnel ε_x and the relative displacement of flexible joint δs are obtained as follows;

$$\varepsilon_x = \gamma_{xx} \left\{ 1 - \frac{\cosh \beta x}{\beta \ell} \left(1 - \frac{2 \dfrac{\tanh \dfrac{\beta \ell}{2}}{\beta \ell}}{\dfrac{EA}{k_j \ell} + \dfrac{2 \tanh \dfrac{\beta \ell}{2}}{\beta \ell}} \right) \right\} \quad \cdots\cdots\cdots (4)$$

$$\delta s/\ell = \gamma_{xx} \frac{\frac{2}{\beta\ell}\tanh\frac{\beta\ell}{2}}{1 + \frac{k_j\ell}{EA}\frac{2\tanh\frac{\beta\ell}{2}}{\beta\ell}} \quad \cdots\cdots\cdots \quad (5)$$

$$\beta = \sqrt{\frac{K_x}{EA}}$$

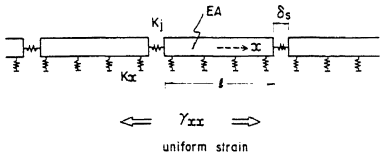

Fig. 10 Simplified Numerical Model

where EA and ℓ are the stiffness of push-pull deformation and the length of the tunnel element, while k_j and k_x are the srping constant of the flexible joint and the coefficient of the subgrade reaction. γ_{xx} is the normal strain of the ground in the axial direction.

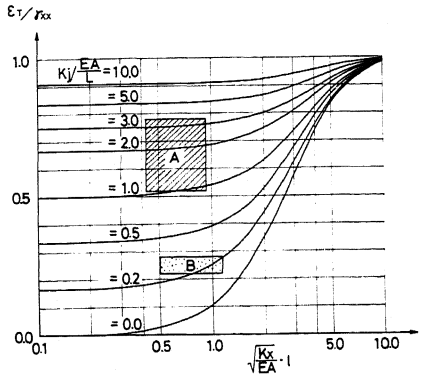

Fig. 11 Strain Transfer Ratio

Fig. 11 shows the ratio of the maximum strain of the tunnel to the ground strain (strain transfer ratio) which is obtained by substituting x = 0 into Eq. (4) and Fig. 12 shows non-dimensional relative displacement of joints. From these figures it is clarified that the strain transfer ratio is always less than 1.0 and the relative displacement of the joint is smaller than $\gamma_{xx}\ell$.

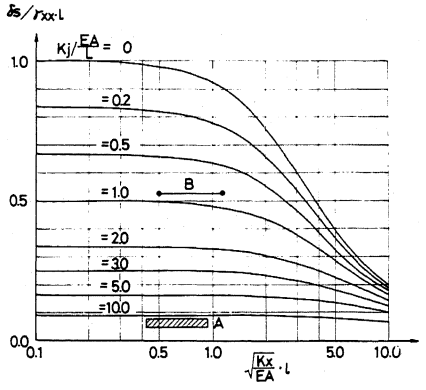

Fig. 12 Non-Dimensional Relative Displacement of Joint

Examination of Flexibility of Joints

Table 1 shows the maximum strain transfer ratio and maximum non-dimensional relative displacement of joints observed on the two tunnels during Izu and Chiba-Earthquakes. The apparent phase velocities along tunnel axes in the table were ontained from the time lag at two observation points and the non-dimensional parameter $\beta\ell$ was estimated as 0.42 ∿ 0.94 for A-tunnel and 0.50 ∿ 1.12 for B-tunnel on the assumption that the coefficient of the subgrade reaction in the axial direction was 0.1 ∿ 0.5 kg/cm/cm^2.

The shadow area in Fig. 11 and 12 shows the probable zones of the ratio of the joint spring K_j to the stiffness of tunnel elements EA/ℓ. There are some difference between the zone indentified from the maximum strain of the tunnel (Fig. 11) and the one indentified from the maximum relative displace-

Tunnel	A (ℓ = 110 m)		B (ℓ = 124 m)	
$\sqrt{\frac{k_x}{EA}} \cdot \ell$ (Assumed)	0.42 ~ 0.94		0.50 ~ 1.12	
Earthquake	Chiba	Izu	Chiba	Izu
Max. Strain of Tunnel ε_T	5.4×10^{-6}	5.0×10^{-6}	4.4×10^{-6}	2.5×10^{-6}
Max. Relative Disp of Joint δ_s (mm)	0.061	0.053	≒ 1.04	—
Max. Axial Particle Velocity V_x (cm/sec)	2.9	1.1	6.7	4.8
Max. Apparent Phase Vel. v_x (m/sec)	2800	1720	4200	2200
Max. Ground Strain $\gamma_{xx} = \frac{V_x}{v_x}$	10.4×10^{-6}	6.4×10^{-6}	16.0×10^{-6}	21.6×10^{-6}
Strain Ratio $\frac{\varepsilon_T}{\gamma_{xx}}$	0.52	0.78	0.28	0.22
Relative Disp. Ratio $\frac{\delta_s}{\gamma_{xx} \cdot \ell}$	0.05	0.08	0.53	—

Table 1 Strain Transfer Ratio and Relative Displacement of Joints Observed on Two Tunnels during chiba and Izu-Earthquakes

ment (Fig. 12). However, it can be understood that the ratio of the joint spring to the stiffness of the tunnel element is much larger in A-tunnel than in B-tunnel. This is a reasonable result by considering that B-tunnel has much more flexible joints which were fabricated by only P.C. cables than A- tunnel the joint of which was by steel shear keys and mortar concrete.

CONCLUSION

By the inspection of earthquake records of two submerged tunnels in Tokyo Port and some numerical considerations on the deformation characteristics of the tunnels, the followings were obtained as the main results;

(a) The strain due to the push-pull deformation in the axial direction is larger than that due to the bending deformation around the vertical axis. Particularly, the axial strain is dominant during an earthquake with long period vibration component.

(b) The axial and the bending strains have a close relationship with the velocity and the acceleraration of the earthquake motion, respectively.

(c) The flexibility of the joints between tunnel elements has a great effectiveness on the reduction of the tunnel strain.

REFERENCE

(1) Tamura, C., Okamoto, S. and Hamada, M. (1975) Dynamic Behavior of A submerged Tunnel during Earthquakes, Report of the Institute of Industrial Science, The University of Tokyo, vol. 24, No. 5, March.